
This is an electronic reprint of the original article.
This reprint may differ from the original in pagination and typographic detail.

Zhou, Liang; Tirkkonen, Olav; Parts, Ulo; Khosravirad, Saeed R.; Baracca, Paolo; Korpi, Dani; Uusitalo, Mikko

Dual-mode Ultra Reliable Low Latency Communications for Industrial Wireless Control

Published in:
2022 IEEE 95th Vehicular Technology Conference - Spring, VTC 2022-Spring - Proceedings

DOI:
[10.1109/VTC2022-Spring54318.2022.9860905](https://doi.org/10.1109/VTC2022-Spring54318.2022.9860905)

Published: 01/01/2022

Document Version
Peer-reviewed accepted author manuscript, also known as Final accepted manuscript or Post-print

Please cite the original version:
Zhou, L., Tirkkonen, O., Parts, U., Khosravirad, S. R., Baracca, P., Korpi, D., & Uusitalo, M. (2022). Dual-mode Ultra Reliable Low Latency Communications for Industrial Wireless Control. In *2022 IEEE 95th Vehicular Technology Conference - Spring, VTC 2022-Spring - Proceedings* (IEEE Vehicular Technology Conference). IEEE. <https://doi.org/10.1109/VTC2022-Spring54318.2022.9860905>

Dual-mode Ultra Reliable Low Latency Communications for Industrial Wireless Control

Liang Zhou¹, Olav Tirkkonen², Ülo Parts¹, Saeed R. Khosravirad³, Paolo Baracca⁴, Dani Korpi⁵, Mikko Uusitalo⁵

¹ Inalambrica Oy, Helsinki, Finland,

² Aalto University, Finland,

³ Nokia Bell Labs, Murray Hill, NJ, USA,

⁴ Nokia Bell Labs, Stuttgart, Germany,

⁵ Nokia Bell Labs, Espoo, Finland

e-mail: liang.zhou-l1witec@protonmail.com, olav.tirkkonen@aalto.fi, firstname.lastname@nokia-bell-labs.com

Abstract—This paper studies communications service availability for industrial wireless control systems. We consider a motion controller with a continuous closed-loop control link to a group of actuator devices on a factory floor. The goal is to satisfy *end-to-end latency* for each packet and to guarantee that the communication service will not be un-available for longer than a *survival time*. We propose to decouple the scheduling operation between the normal and survival modes of operation, enabling a *dual-mode* ultra-reliable and low-latency communications (URLLC) scheduler. Scheduler strategies for the survival mode are presented, targeting link adaptation and signal to interference and noise ratio (SINR) estimation in presence of temporal and spatial channel correlation. Through numerical examples, we investigate the impact of channel correlation on the schedulers ability to target the required reliability for each mode. We further present our findings on system-level performance evaluation of such scheduling strategies by adopting a realistic system setup and channel model to obtain insights with high level of realism. Extensive simulation results are presented which demonstrate significant reduction in resource utilization with the proposed dual-mode scheduler when compared to single-mode URLLC scheduling. Specifically, our results demonstrate that the scheduler should target moderate packet error rate (PER) for normal mode of operation and very low PER for the survival mode; the latter guarantees service availability while the former saves radio resources.

Index Terms—IIoT, URLLC, survival time, service availability.

I. INTRODUCTION

A. Industrial Wireless Control

Dependable and secure wireless connectivity in the future industrial internet-of-things (IIoT) will seamlessly and flexibly connect humans and software automated controller with machines and the digital twin of the industrial environment. The wireless transformation is a key factor in the next industrial revolution—dubbed Industry 4.0—by eliminating the need for cumbersome and expensive wire connections and moving towards dynamically re-configurable and flexible industrial environments.

The expectations from wireless communication systems in industrial environments are demanding and in sharp contrast to the requirements for mobile broadband communications—few examples are listed in Table I. Sub-milliseconds end-to-end (E2E) latency and extreme high reliability have been

extensively addressed in research and development activities in the recent years [1]–[5]. In the meantime, other new quality of service (QoS) characteristics for industrial wireless control, including survival time, didn't receive the same attention.

B. New QoS Characteristics

The more distinct aspect of those requirements, introduced by 3rd generation partnership project (3GPP) for 5G and beyond wireless control, is the new notion of survival time [6]. The terminologies in Table I are defined according to the interaction between the control application and the wireless communications system, as follows:

a) *Transfer interval*: is the time difference between arrival of two consecutive packet from the application to the wireless communications system.

b) *Survival time*: is the time that an application consuming a communication service may continue without an anticipated message. The anticipation is typically due to the periodic pattern of the traffic.

c) *Communication service availability*: is the fraction of time the E2E communication service QoS requirements are satisfied—this includes E2E latency and survival time requirements. In Table I, communication service outage is presented, defined as the remaining fraction of time where those requirements are not satisfied.

The duration of the survival time is variant depending on the application. For high precision motion control applications, it is comparable to one transfer interval, while for less stringent operation accuracy, such as control of a harbor crane, it may be as large as six consecutive transfer intervals [7].

C. Motivations for Dual-mode Transmissions

The immediate impact of introducing survival time as a QoS requirement of the wireless link is a shift in design paradigm from typical link reliability to service availability. Instead of minimizing PER in conventional design, the system with survival time should try to minimize the chance of a burst of consecutive errors. In theory excellent service availability can be achieved even with high PER when errors are not consecutive. Two typical examples are illustrated in Fig. 1. The upper left part and lower left part of Fig. 1 depicts examples

TABLE I: QoS characteristics for motion control and haptic feedback [6].

Communication service outage	E2E latency	Message size [byte]	Transfer interval	Survival time	number of devices	Service area	Application
$10^{-7} - 10^{-5}$	< transfer interval	50	500 μ s	500 μ s	≤ 20	50 m \times 10 m \times 10 m	Motion control
$10^{-8} - 10^{-6}$	< transfer interval	N/A	≤ 1 ms	3 \times transfer interval	2-5	100 m \times 30 m \times 10 m	Wired-2-wireless 100 Mbps link replacement
10^{-8}	< 2 ms	50	2 ms	2 ms	> 2	100 m ²	Mobile Operation Panel: Haptic feedback data stream

with the same PER but different service availability. In the upper example, the service availability is dropped to 0.8 due to consecutive packet errors. In the lower example the service availability is 1 even with four packet errors which are not consecutive.

Specifically, in presence of a reliable feedback channel that promptly reports the occurrence of packet failure, the relaxation on link reliability requirement can be more meaningful [8]. An intelligent wireless scheduler can then differentiate between *survival mode*, i.e., a mode where the last packet has failed, and a *normal mode* of operation, and take advantage of such relaxed PER requirement to increase the overall resource utilization efficiency, hence, enabling *dual-mode* transmission for efficient service availability, which would otherwise be inaccessible in absence of reliable feedback.

D. Prior Work

To reduce the chance of consecutive packet failures, different approaches have been proposed in the literature. In [9], it is proposed to exploit spacial diversity by consistently alternating transmissions among different base stations (BSs) with independent channels to the user. This requires base stations to continuously cooperate in transmissions, even when there is no packet error. In [10], it is suggested to use network coding to reduce the chance of single and consecutive errors caused by simultaneous failures over multiple radio links. The work in [11] presents a simulation analysis on the impact of different resource allocation schemes, suggesting a conservative link-adaptation for a link in survival mode. Different from the present article, the work in [11] does not differentiate between the survival and normal modes of operation.

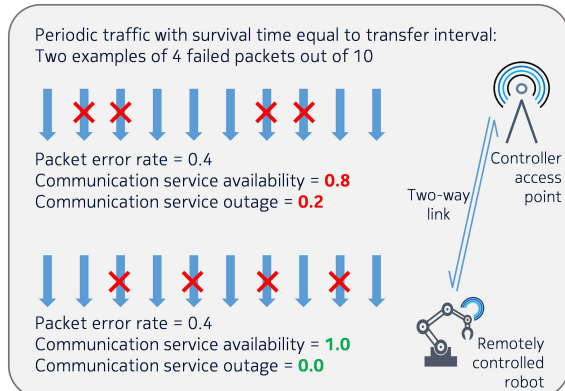


Fig. 1: Service availability vs link reliability: two examples of packet streams with equivalent number of packet failures resulting in contrasting service availability measures.

Analysis of service availability for periodic traffic has recently gained attention in the literature. In [12], the statistics of service availability time is characterized in the absence of wireless channel statistics and channel state information.

E. Contributions

In this paper we propose a novel wireless scheduling framework for applications with stringent service availability requirements. Extensive system-level performance evaluation of such scheduling framework are performed with high level of realism. The contributions of this paper are listed as follows:

- We propose a dual-mode scheduler for wireless communications with stringent service availability, differentiating between normal mode and survival mode of operation with decoupled target packet error rate for each mode. The proposed framework proves to be significantly more efficient in utilizing the radio resources, when compared against typical single-mode ultra-reliable low-latency communications (URLLC) scheduler.
- We analyze the impact of channel temporal correlation on variations of SINR. Moreover, we use extensive simulation analysis to examine the performance of the proposed scheduler framework. We investigate those using dynamic system-level simulations with standard channel models and commonly accepted methodologies, to obtain mature results with high level of realism.
- We present conclusive insights into scheduler design for industrial wireless control systems. Specifically, we show that the scheduler should target moderate PER for normal mode of operation, while reserving very low PER transmission for the survival mode—the latter guarantees service availability while the former saves up radio resources. Moreover, the scheduler should account for the variation of signal to noise ratio (SNR) from the estimation time, by selecting the median rather than the best of the resource blocks for resource allocation.

F. Organization of the Paper

The sequence of the paper is as follows: Sec. II introduces the proposed dual-mode scheduling framework; Sec. III describes the system model and evaluation methodology; Sec. IV investigates the impact of channel temporal correlation on SINR variations; Sec. V presents the system-level simulation results; finally, Sec. VI extends the discussion around the system-level analysis and covers the concluding remarks.

II. DUAL-MODE COMMUNICATIONS

By differentiating between the scheduling settings in normal and survival mode transmissions, the dual-mode scheduling

framework can efficiently achieve the desired consecutive packet error rate (CPEP) for downlink. As introduced in [8], target service availability can be achieved with a trade-off between normal mode error rate and survival mode error rate, which may be utilized to reduce resource usage.

A. Single-mode vs Dual-mode Wireless Scheduler

From the point of view of a typical *single-mode* scheduler, all packets transmitted over the same communications link have equal importance. Thus, the scheduler is designed for satisfying requirements that are averaged over all the packets. For instance, with eMBB traffic the goal is usually to improve spectral efficiency which is achieved by targeting BLER of 0.1 together with flexible HARQ. On the other hand, for many URLLC use cases, the goal is to achieve reliable communications within a limited latency budget. For specific URLLC use cases with survival time requirement, for instance the examples in Table I, it is further required to limit the rate of consecutive packet losses that last for longer than the survival time. While burst consecutive failures not longer than the survival time is allowed.

Therefore, the scheduler's task is to determine the order in which the resources are allocated to the users in the service area. In other words, importance of a packet is impacted by the status of the previous packet in the communications pipeline, thus, suggesting a *dual-mode* scheduler. The scheduler's goal is to reduce the probability for consecutive errors and also use the resources efficiently. It has been shown in [13] that finding the optimized usage of resources is NP hard. That is not practical solution for simulations as the needed time is becoming long to achieve good accuracy with PER levels as low as 10^{-7} . In the simulations we adapt methodology discussed in [11].

B. Scheduling Algorithm

The input of the scheduler is the estimated SINRs of physical resource blocks (PRBs) for each user. Based on that the scheduler calculates the number of expected bits which can be successfully delivered using the PRBs. Channel conditions during transmission are different compared to the time of measurement. Therefore, back-off as scheduling parameter is subtracted from SINR before the calculations. With back-off, the scheduler assumes that the channel will be worse than the estimated channel. In the simulations we use different back-off factor for users in survival and normal mode as reliability requirements are different.

The survival mode users are scheduled first. Within the group the user with maximum weight is selected to allocate a PRB. The weight depends on the average SINRs γ_a of free PRB and on the number of bits b_R still need to be allocated to the user. The weight is a function of γ_a and b_R and its value is larger with larger b_R and smaller γ_a . The scheduler allocates one PRB at the time and full PRB is always allocated to only one user in the serving BS.

The selection of PRBs is determined by resource preference, i.e., PRB with the best or median SINR in the previous slot. Depending on the channel correlation, the PRB with best SINR

TABLE II: Simulation parameters

Parameter	Value
Packet size	50 Byte
Transfer interval	0.5 ms
Bandwidth	30 MHz
BS Tx power	23 dBm
Carrier frequency	1.3 GHz
Maximum bits per PRB	582
BS height	5 m
UE height	2 m
UE speed range	0-22m/s
TDL type(LOS)	TDL-E
TDL type(NLOS)	TDL-C
Pathloss model	InF-SL
Delay spread	6 ns
Thermal noise	-174 dBm/Hz
Noise figure	9 dB
Receiver purity noise	-25dB
Noise floor	-30 dB
Background inference	-149 dBm/Hz
Subcarrier frequency	15kHz

in the previous slot should have higher mean value of SINR, which indicates that in average more bit can be allocated. However, it is risky to apply greedy bit allocation according to SINR in the previous slot because the SINR drop in present slot may increase packet error rate.

Once the PRB is allocated, the weights are re-calculated as the number of free PRBs is smaller by 1 and b_R for that user is smaller as well. The allocation proceeds until all users get enough resources or all PRBs are used.

III. SIMULATION SETTING

In order to simulate consecutive error cases in practical environment, extensive system-level simulations are constructed with assumptions which try to describe realistic feature of system components. The main simulation parameters are shown in Table II.

A. Simulation Structure

The statistics are collected from about 10^5 simulation instances. Each instance simulate wireless channels with a time slice of 25 ms. At start of an instance, the position and speed of UEs are randomly initialized. Then the downlink communication is simulated with TI = 0.5 ms. In each TI, the scheduler allocates radio resources according to estimated SINR from previous TI. The SINR on allocated resource at UE receiver is evaluated to estimate whether packets can be successfully received. PER and consecutive packet error rate (CPEP) incidents are monitored for the duration of the instance. The reported statistics of PER and CPEP in the following are therefore result of simulating 5×10^6 number of TI in aggregate.

B. Factory Model

An indoor factory environment is modeled according to [14]. The factory layout for simulations is depicted in Fig. 2, demonstrating four BSs symmetrically located in a $100 \times 100 m^2$ factory with 5 m height to the ground and 25 m distance to the nearby walls. In each simulation instance, UEs are randomly dropped in horizontal area of the factory with 2 m

height. It is assumed that UEs move towards random directions with constant moving speed which is randomly selected from within the range of 0-22 m/s. BSs and UEs are equipped with single-antenna transceivers.

C. Network Resource Allocation

Considering low signal attenuation at short distance, we applied frequency reuse 4 to avoid interference from nearby BSs. The resources are proportionally allocated among four BSs depending on number of served UE for each BS. With single node transmission, each BS does not transmit on the resources belong to other BSs.

D. Channel Model

The pathloss model is constructed according to indoor factory scenario 'InF-SL' in [14], where line-of-sight (LOS) or non-line-of-sight (NLOS) model is randomly selected according to a probability calculated from horizontal distance between transmitter and receiver. The shadow fading values are also generated according to the scenario with correlation distance $d_{cor} = 10$ m, which specifies the correlation function that describes the correlation between adjacent shadow fading values in [14]. For simplicity, the fast fading is formulated with Jakes's model. When simulating channel impulse response for each TI, we apply Tapped Delay Line (TDL) models from [14], which includes 'TDL-C' for NLOS cases and 'TDL-E' for LOS cases. The RMS delay spread is set to 6 ns [15]. For LOS case, the phase of LOS component is updated according to UE's position in each TI.

E. SINR Calculation

To simulate practical SINR measurements, four types of noise are considered in SINR calculation: background noise n_b , receiver purity noise n_r , channel estimation error e_h and noise floor n_f . The background noise power is calculated by total mean power of thermal noise and background interference, which is estimated with six interfering source at 100 m distance. The power of n_r is 25 dB weaker than received signal power. The channel of one pilot \hat{h}_p is estimated with received pilot y_p and transmitted pilot x_p

$$\hat{h}_p = \frac{y_p}{x_p} = h + \frac{n_b}{x_p} = h + e_p, \quad (1)$$

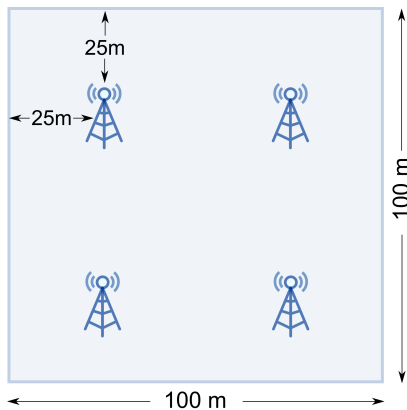


Fig. 2: Factory layout

where h is channel coefficient and e_p is channel estimation error of one pilot. The estimated channel \hat{h} is averaged value of \hat{h}_p through two pilots per PRB per slot. Given estimated channel $\hat{h} = h + e_h$, the equalized signal \hat{x} is

$$\hat{x} = \frac{y}{\hat{h}} = \frac{hx + n}{h + e_h} = x + \frac{-xe_h + n}{h + e_h} = x + \hat{e}, \quad (2)$$

where y is received signal, x is transmitted signal, $n = n_b + n_r$, \hat{e} is the error after equalization. To simulate non-linear noise, the SINR γ is calculated with noise floor n_f

$$\gamma = \frac{|x|^2}{|\hat{e}|^2 + |n_f|^2}, \quad (3)$$

where $|n_f|^2 = \frac{|x|^2}{1000}$.

F. Packet Transmission

Utilizing the algorithm introduced in Sec. II-B, scheduler allocates PRBs according to specified resource preference with corresponding transmission rates, which are estimated according to previous SINR of PRBs and chosen back-off SINR. The Shannon capacity of the received SINR for allocated PRBs is calculated and compare to packet size. If the capacity of allocated PRBs is larger than the transmission rate, the packet reception is considered to be successful.

IV. NUMERICAL ANALYSIS FOR CHANNEL VARIATION

Packet error usually occurs when channel is worse than expected. Therefore it is important to study channel variation for URLLC applications. The cumulative density function (CDF) of SINR variation for different selection of PRBs are depicted in Fig. 3. The horizontal axis represent the SINR variation. For a UE u , the SINR variation on PRB n in slot i is defined as

$$v_{u,i}^n = 10 \log_{10} \frac{\gamma_{u,i}^n}{\gamma_{u,i-1}^n} \quad (4)$$

where $\gamma_{u,i}^n$ is the SINR measured on PRB n in slot i . In Fig. 3, the blue curves illustrate the CDF of SINR variation for all PRBs. From the blue curves we can estimate probability of channel fading in general. For example, at 0 dB the CDF value for blue curve is 0.5, which means that, as expected, there is 50% probability that channel will get worse in next slot. From this blue curve we can estimate the error probability in case the scheduler randomly pick up a PRB for a UE and use corresponding back-off SINR on horizontal axis to derive scheduling SINR from the estimated SINR. This is referred to random PRB preference. The error probability with 10 dB back-off is equal to probability of a randomly selected PRB suffering a fading that causes a SINR drop larger than 10 dB, which is value of CDF at -10 dB SINR variation. The red curve in Fig. 3 illustrates the SINR variation of the PRBs which have the best SINR in corresponding slots. From this red curve we can estimate the error probability in case the scheduler pick up the PRB with the best SINR for a UE, which is referred to best PRB preference for scheduler. Similarly, the yellow curve in Fig. 3 illustrates the SINR variation of the PRBs with median SINR in corresponding slots, which is

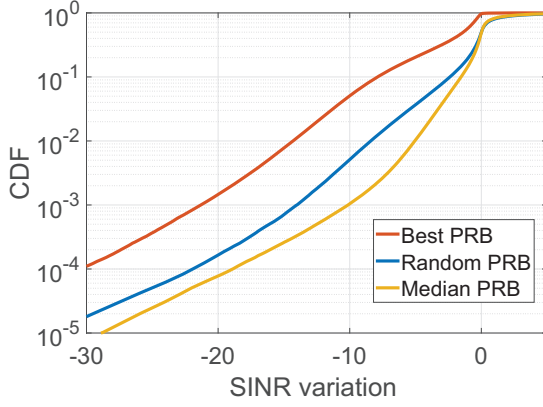


Fig. 3: SINR variation for specified PRBs.

related to median PRB preference. It can be observed that, targeting at same error rate, best PRB preference may require much higher back-off SINR than random PRB preference. For feasible SINR variation which is larger than -40 dB, median PRB preference require a bit less back-off SINR than choosing random PRBs. Considering both capacity and reliability of the PRB, the median PRB preference is probably better choice for URLLC type applications.

In Fig. 3 the CDF of SINR variation is illustrated, which could be used to estimate target packet error rate in the normal mode (P_n) given the estimated SINR, the selected back-off, and the PRB preference. In order to estimate target packet error rate in the survival mode (P_s), it is necessary to collect statistics of the conditional SINR variation in survival mode. The cdf of conditional SINR variation conditioned by previous SINR variation on the same PRB is depicted in Fig. 4. This figure reveals channel correlation between consecutive slots. It can be observed that, when the same PRB is scheduled for normal mode and survival mode, the most risky zone of normal mode back-off SINR is around -15 dB. This indicate that when channel fade around -15 dB, there is a higher probability that the same channel would experience deep fading also in consecutive slot. Such behavior must be considered in the design of an intelligent scheduler.

In practical cases scheduler does not always allocate same resources to UE, therefore it is necessary to study the correlation between different resources among consecutive slots. Fig. 5 illustrates the CDF of conditional SINR variation on specified resources conditioned by maximum SINR variation with best PRB preference in the previous slot. The figure reveals the correlation between different resources from consecutive slots. Curves in Fig. 5 can be used to estimate the survival mode error probability with corresponding resource preference of survival mode, given best PRB preference in normal mode. The resource preference combination with **best** PRB preference in normal mode and **best** PRB preference in survival mode is abbreviated to “**best to best**” or “**BtoB**”, similarly for “**BtoM**”, etc. For example, if 24 dB back-off SINR is applied in normal mode, the blue solid curve can be used to estimate the packet error rate of survival mode with resource preference combination BtoB. It can be observed that when best PRB is chosen for survival mode, the error rates

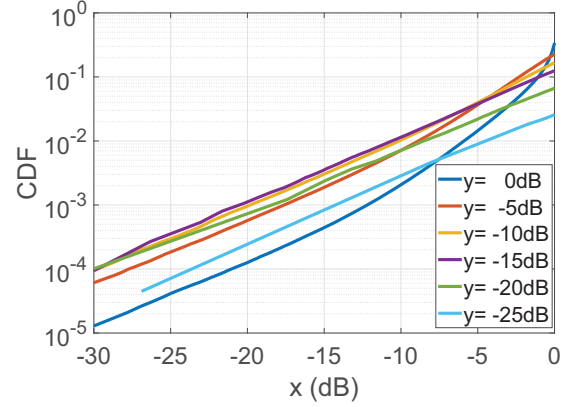


Fig. 4: Conditional SINR variation on the same PRB conditioned on SINR variations on same PRB in previous slot. CDF function $F_{v_{u,i}^{n_i}}(x) = P(v_{u,i}^{n_i} < x | v_{u,i-1}^{n_{i-1}} < y)$, where $n_{i-1} = n_i$.

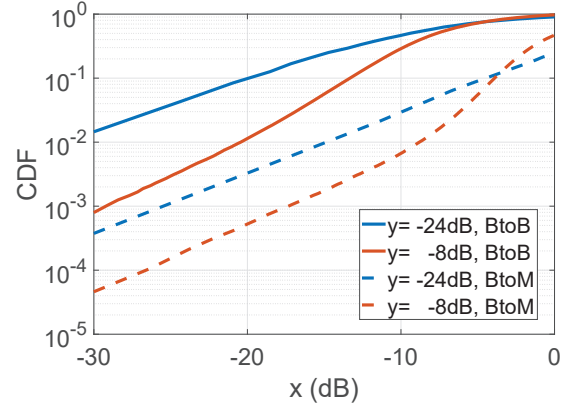


Fig. 5: Conditional SINR variation on selected PRBs conditioned on SINR variations on best PRB in previous slot. CDF function $F_{v_{u,i}^{n_i}}(x) = P(v_{u,i}^{n_i} < x | v_{u,i-1}^{n_{i-1}} < y)$, where n_{i-1} is the best PRB in slot $i-1$. For BtoB: n_i is the best PRB in slot i . For BtoM: n_i is the median PRB in slot i .

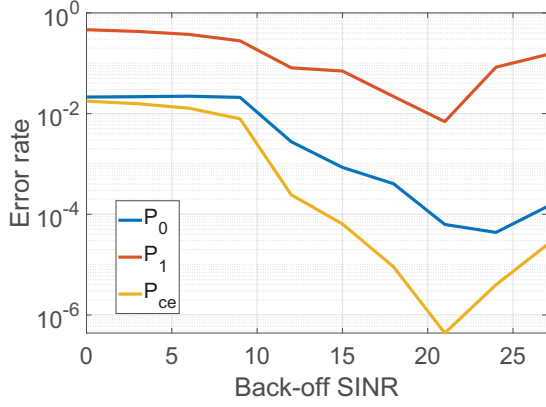
of survival mode is much higher than choosing median or random PRB in survival mode. The curves of the random PRB preference and median PRB preference are reasonably similar.

Note that the estimate for different resource preference is approximately close only when one resource block is needed for each packet. With higher back-off, the estimate is not accurate since multiple PRBs are needed for packet transmission.

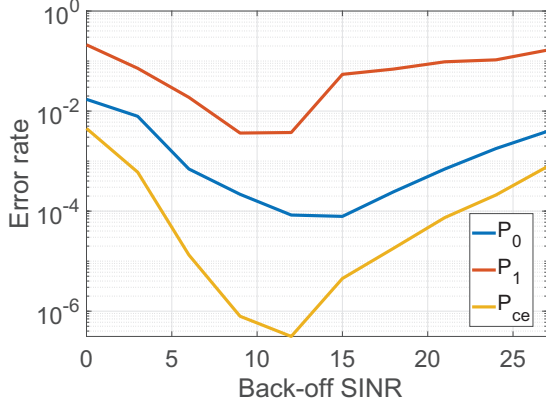
V. NUMERICAL ANALYSIS FOR RESOURCE PREFERENCE

A. Single-mode Scheduler

The single-mode scheduler is simulated by assuming all UEs are served only in normal mode with same back-off SINR and resource preference. The measured error rates with best PRB preference and median PRB preference are depicted in Fig. 6a and Fig. 6b separately. The blue curves represent the conditional packet error rate P_0 conditioned on the previous packet being successful, while the red curves represent the conditional packet error rate P_1 conditioned on



(a) Error rate with best PRB preference.



(b) Error rate with median PRB preference.

Fig. 6: Error rates with single-mode scheduler as function of back-off SINR. Total 10 UEs and 150 PRBs.

the failure of the previous packet. The yellow curve represent the consecutive packet error rate $P_{ce} = P_0 * P_1$. Evidently, $P_1 > P_0$ in both figures, which also indicates the high chance of consecutive deep fade occurrence.

In Fig. 6a, error rates vary very little with back-off SINR range from 0 to 8 dB. This feature can usually be observed with best PRB preference. Due to the fact that scheduler allocates resources with PRB granularity, it is likely that the scheduled resources with high SINR can fit more bits than the intended packet size, thus further reducing the effective rate of the transmission and emulating a hidden back-off. This hidden back-off also explains why P_0 is as small as 10^{-2} level even when back-off SINR is zero. As back-off SINR increases, all error rates first descend to the minimum then ascend. This is because as back-off SINR increases, error rates decrease while resource usage increases. Once back-off SINR is so large that available resources are not sufficient to schedule all users, error rates start to increase again. The minimum P_{ce} is about 4×10^{-7} with 21 dB back-off SINR.

In Fig. 6b, P_{ce} reaches about 3×10^{-7} when back-off SINR is 12 dB. Compared to Fig. 6a, with median PRB preference lower consecutive packet error rate can be achieved with smaller back-off SINR and less resource utilization. This confirms the importance of resource preference for the scheduler when accounting for the variation of SINR from the

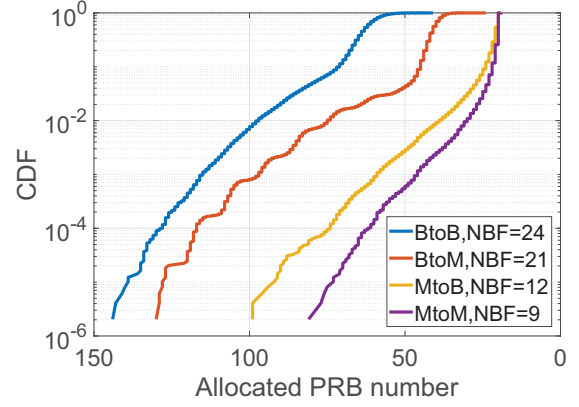


Fig. 7: Resource usage comparison between different resource preferences with SBF = 0 dB, $P_{ce} = 2.2 \times 10^{-5}$ (BtoB), 3.1×10^{-5} (BtoM), 2.1×10^{-5} (MtoB), 1.1×10^{-5} (MtoM). Total 10 UEs and 150 PRBs.

estimation time.

B. Dual-mode Scheduler

Fig. 7 depicted resource utilization of different resource preferences, which achieve roughly same P_{ce} with 0 dB survival mode back-off SINR (SBF) and corresponding normal mode back-off SINR (NBF). With such biased back-off setting P_{ce} is achieved with high survival mode error rate P_s and low normal mode error rate P_n . It can be observed that resource usage highly depends on back-off SINR and resource preference of normal mode. The upper part of CDF curves reflect normal mode, which is the most often serving mode for the users, while the lower part reflects the survival mode. The blue curve and red curve share the similar shape for upper part due to same resource preference applied in normal mode, so do the rest two curves. It is shown that the resource preference “MtoM” achieves the lowest P_{ce} with the least resource utilization, which is at least 20 PRBs.

Resource usage of different resource preference modes are compared in Fig. 8, where roughly same P_{ce} is achieved with 0 dB NBF and corresponding SBF values. This back-off setting indicates high P_n with low resource usage, i.e., 10 PRBs, in normal mode and low P_s with high resource usage in survival mode. As UEs are mostly served in normal mode, it is more efficient to select greedy scheduling in normal mode to improve mean resource usage, while the P_{ce} is guaranteed by utilizing conservative scheduling in survival mode using a larger SBF. At low percentiles of CDF, similar shapes can be observed where the same resource preference is applied in survival mode, i.e., blue and red curves. Considering SBF values, “BtoM” and “MtoM” can achieve specified P_{ce} level with smaller SBF than other two preferences.

Fig. 9 compares the resource usage of single-mode and dual-mode scheduling, where approximate same P_{ce} is achieved with corresponding back-off SINR and resource preference. The CDF of resource allocation for single-mode scheduling with 8 dB back-off SINR is depicted as red curve. The blue curve is CDF of resource allocation for the dual-mode settings, which applies 0 dB NBF to save resources and 16 dB SBF

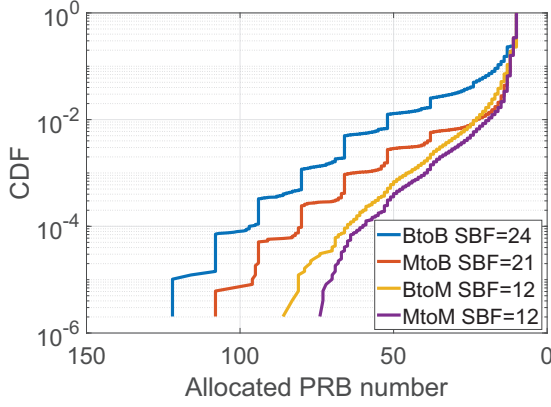


Fig. 8: Resource usage comparison between different resource preferences with NBF = 0 dB, $P_{ce} = 3.6 \times 10^{-5}$ (BtoB), 2.4×10^{-5} (MtoB), 1.7×10^{-5} (BtoM), 1.9×10^{-5} (MtoM). Total 10 UEs and 150 PRBs.

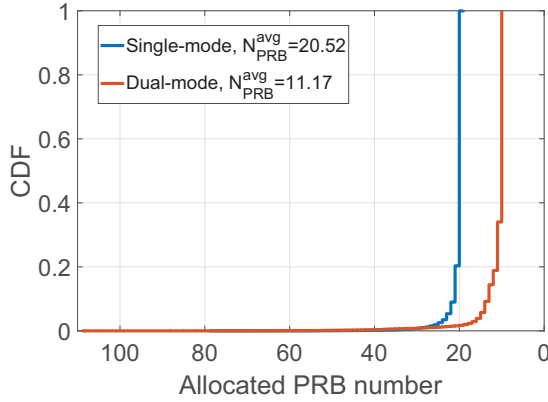


Fig. 9: Resource usage comparison between single-mode and dual-mode scheduler. Single-mode: median PRB preference, BF = 8 dB, $P_{ce} \approx 2.5 \times 10^{-6}$, the average PRB usage $N_{PRB}^{avg} = 20.52$. Dual-mode: MtoM, NBF = 0 dB, SBF = 16 dB, $P_{ce} \approx 2.3 \times 10^{-6}$, the average PRB usage $N_{PRB}^{avg} = 11.17$. Total 10 UEs and 150 PRBs.

to improve P_{ce} . The blue curve reaches the approximately same P_{ce} with about 45% less average resource usage, which indicates almost 2 times efficiency on usage of radio resources with dual-mode scheduling: select median PRB preference with low NBF in normal mode to reduce the resource usage and select median PRB preference with high SBF in survival mode to achieve target service availability. The combination of very low NBF and very high SBF needs a very small amount of resource most of the time but occasionally requires a larger amount of resource. Therefore, for the benefit of resource efficiency to be realized in practice, the wireless scheduler should enable flexible resource sharing among applications at the system level and on-demand access to larger resources for critical traffic.

VI. CONCLUSION

In this paper, we propose a dual-mode scheduler for wireless applications with stringent service availability requirement. We analyze and simulate the impact of channel temporal

correlation on variation of SINR for those applications. It is shown that if specific SINR drop leads to a first transmission error, there is increased probability of a very weak channel during the following transmission. It is demonstrated that selecting resources with the median PRB preference is more efficient than with best PRB preference for both single-mode and dual-mode URLLC type applications. The simulation results shows that, differentiating settings between normal mode and survival mode, dual-mode scheduler can achieve same service availability with about 84% improvement in resource efficiency compared to typical single-mode URLLC scheduler.

ACKNOWLEDGMENT

This work was supported in part by the Finnish public funding agency for research, Business Finland under the project “5G VIIMA”, grant number 6430/31/2018. 5G VIIMA is part of 5G Test Network Finland (SGTNF). The work of OT was funded in part by the Academy of Finland (grant 319484).

REFERENCES

- [1] M. Weiner, M. Jorgovanovic, A. Sahai, and B. Nikolić, “Design of a low-latency, high-reliability wireless communication system for control applications,” in *Proc. IEEE ICC*, 2014, pp. 3829–3835.
- [2] R. Adeogun, G. Berardinelli, P. E. Mogensen, I. Rodriguez, and M. Razzaghpour, “Towards 6G in-X subnetworks with sub-millisecond communication cycles and extreme reliability,” *IEEE Access*, vol. 8, pp. 110 172–110 188, 2020.
- [3] N. Brahmi, O. N. C. Yilmaz, K. W. Helmersson, S. A. Ashraf, and J. Torsner, “Deployment strategies for ultra-reliable and low-latency communication in factory automation,” in *Proc. IEEE GLOBECOM Workshops*, 2015, pp. 1–6.
- [4] V. N. Swamy, S. Suri, P. Rigge, M. Weiner, G. Ranade, A. Sahai, and B. Nikolić, “Cooperative communication for high-reliability low-latency wireless control,” in *Proc. IEEE ICC*, 2015, pp. 4380–4386.
- [5] S. R. Khosravirad, H. Viswanathan, and W. Yu, “Exploiting diversity for ultra-reliable and low-latency wireless control,” *IEEE Trans. Wireless Comm.*, in press.
- [6] 3GPP, “Service requirements for cyber-physical control applications in vertical domains; Stage 1,” Tech. Rep. TS 22.104, v. 17.4.0, Sep. 2020.
- [7] H. Kokkonen-Tarkkanen et al., “Enabling safe wireless harbor automation via 5G URLLC,” in *IEEE 5G World Forum (5GWF)*, 2019, pp. 403–408.
- [8] O. Tirkkonen, S. R. Khosravirad, P. Baracca, L. Zhou, U. Parts, D. Korpi, and M. A. Uusitalo, “Optimized survival mode to guarantee QoS for time-critical services,” in *Proc. IEEE ICC Workshops*, 2021, pp. 1–6.
- [9] J. Gebert and A. Wich, “Alternating transmission of packets in dual connectivity for periodic deterministic communication utilising survival time,” in *Proc. EuCNC*, 2020, pp. 160–164.
- [10] S. Paris, P. Kela, D. Laselva, and Q. Zhao, “Addressing reliability needs of industrial applications in 5G NR with network coding,” in *Proc. IEEE VTC Spring*, 2020, pp. 1–6.
- [11] J. Demel, C. Bockelmann, and A. Dekorsy, “Burst error analysis of scheduling algorithms for 5G NR URLLC periodic deterministic communication,” in *Proc. IEEE VTC Spring*, 2020, pp. 1–6.
- [12] S. Samarakoon, M. Bennis, W. Saad, and M. Debbah, “Predictive ultra-reliable communication: A survival analysis perspective,” *IEEE Comm. Lett.*, vol. 25, no. 4, pp. 1221–1225, 2021.
- [13] A. Destounis and G. S. Paschos, “Complexity of URLLC scheduling and efficient approximation schemes,” in *2019 International Symposium on Modeling and Optimization in Mobile, Ad Hoc, and Wireless Networks (WiOPT)*, 2019, pp. 1–8.
- [14] 3GPP, “Study on channel model for frequencies from 0.5 to 100 GHz,” Tech. Rep. TS 38.901 v16.1.0, 2019.
- [15] S. Jaeckel, N. Turay, L. Raschkowski, L. Thiele, R. Vuonttoniemi, M. Sonkki, V. Hovinen, F. Burkhardt, P. Karunakaran, and T. Heyn, “Industrial indoor measurements from 2-6 GHz for the 3GPP-NR and QuaDRiGa channel model,” in *Proc. IEEE VTC Fall*, 2019, pp. 1–7.